Fission yeast Dna2 is required for generation of the telomeric single-strand overhang

Kazunori Tomita[1,4], Tatsuya Kibe[1], Ho-Young Kang[2], Yeon-Soo Seo[2], Masahiro Uritani[1], Takashi Ushimaru[3] and Masaru Ueno[1]*

[1]Department of Chemistry, [3]Department of Biology, Shizuoka University, 836 OYA, Shizuoka, 422-8529, Japan

[2] Department of Biological Sciences, Korea Advanced Institute of Science and Technology 373-1 Kusung-Dong, Yusung-Ku, Daejeon, 305-701, Korea

[4] Present address: Telomere Biology Laboratory, Cancer Research UK 44 Lincoln's Inn Fields, London EC2A 3PX, UK

Running head: Dna2 generates telomeric single-strand overhang

* Correspondence. Mailing address: Department of Chemistry, Faculty of Science, Shizuoka University, 836 OYA, Shizuoka 422-8529, JAPAN

Phone: +81-54-238-4762 Fax: +81-54-237-3384. Email: scmueno@ipc.shizuoka.ac.jp

Abstract

The *S. pombe* Rad50 (Rad50-Rad32-Nbs1) complex has been suggested to be required for the resection of the C-rich strand at telomere ends in *taz1-d* cells. However, the nuclease-deficient Rad32-D25A mutant can still resect the C-rich strand, suggesting the existence of a nuclease that resects the C-rich strand. Here, we demonstrate that a *taz1-d dna2-2C* double mutant lost the G-rich overhang at a semi-permissive temperature. The amount of G-rich overhang in S phase in the *dna2-C2* mutant was lower than that in wild-type cells at the semi-permissive temperature. Dna2 bound to telomere DNA in a ChIP assay. Moreover, telomere length decreased with each generation after shift of the *dna2-2C* mutant to the semi-permissive temperature. These results suggest that Dna2 is involved in the generation of G-rich overhangs in both wild-type cells and *taz1-d* cells. The *dna2-C2* mutant was not γ-ray sensitive at the semi-permissive temperature, suggesting that the ability to process DSB ends was not affected in the *dna2-C2* mutant. Our results reveal that DSB ends and telomere ends are processed by different mechanisms.

(Introduction)

Telomeres are essential for the stability of eukaryotic chromosome ends (25). Telomeric DNA comprises tandem repeats of a simple sequence rich in guanine residues. Vertebrate telomeres contain regular repeated motifs, TTAGGG. Although the telomeric DNA repeats in *S. pombe* are not completely regular, the most frequent motif can be designated as $(GGTTACA)_n$ (29). The distal end of telomere DNA has a single-stranded region at the 3' end, which is called G-rich overhang. The G-rich overhang is eroded at senescence, suggesting that overhang erosion triggers senescence in cultured primary human cells (51). The G-rich overhangs exist during most of the cell cycle in human cells (36). In contrast, the amount of G-rich overhangs increases in S phase in both *S. cerevisiae* and *S. pombe* (23, 33, 63). It has been suggested that the G-rich overhang is generated by degradation of the C-rich strand (23, 36). However, the nuclease responsible for this activity has not been identified. Although *S. cerevisiae* Est2, which is the telomerase catalytic subunit, binds telomeres throughout the cell cycle, Est1 and Cdc13 bind telomeres mainly in S phase (54). Based on these and other studies, it has been proposed that telomerase synthesizes telomere DNA in late S phase (55).

In *S. pombe*, telomeres are maintained by $trt1^+$, which encode the catalytic subunit of telomerase (41) and are protected by Taz1, which is an ortholog of human TRF1 and TRF2. Deletion of $taz1^+$ causes massive telomere elongation and a significant increase in the amount of G-rich overhang (20, 59). This overhang is detected in *taz1-d*

trt1-d double mutants, suggesting that the G-rich overhang is produced by the degradation of the C-rich strand. The Rad50 (Rad50-Rad32-Nbs1) complex is required for the generation of G-rich overhangs in *taz1-d* cells. However, the nuclease activity of Rad32 is not required for the generation of G-rich overhangs in *taz1-d* cells (59). Therefore, the existence of an additional nuclease that resects telomere end has been predicted.

The Rad50 complex is also involved in the processing of DSB ends. Rad50 has ATP-dependent DNA-binding activity and partial DNA unwinding activity (46, 49). Rad50 stimulates the nuclease activity of Mre11(45, 60). Mre11 (a homolog of *S. pombe* Rad32) possesses 3'-to-5' single and double-stranded exonuclease and single-stranded endonuclease activities, and DNA hairpin opening activity *in vitro* (27, 38, 45, 60, 62). Nbs1(Xrs2) is conserved from *S. cerevisiae* to humans and is believed to be a regulatory subunit of the Rad50 complex (16, 21, 58, 61).

The *S. cerevisiae DNA2* gene was identified as a temperature-sensitive replication mutant (34), and cloned by the complementation of the *dna2ts* gene phenotype (12). Dna2 is a flap-endonuclease that is essential for cell viability and is implicated in Okazaki fragment processing by genetic studies in both *S. cerevisiae* and *S. pombe* (13, 31). Biochemical reconstitution studies suggested that Dna2 participates in the removal of the RNA-containing segments of Okazaki fragments (6), but the exact function of Dna2, if any, in this step remains unclear (5, 30, 32). Both cell biological analysis and a chromatin immunoprecipitation (ChIP) assay showed that *S.cerevisiae* Dna2 is associated with telomeres

in G1 phase (19). In S phase, there is a dramatic redistribution of Dna2 from telomeres to sites throughout the replicating chromosome. Dna2 is again localized to telomeres in late S phase. *S. cerevisiae* Dna2 is also required for *de novo* telomere addition, suggesting that Dna2 is involved in the tight coordination of the lagging-strand replisome with telomerase activity (19).

In this study, we investigated the detailed roles of *S. pombe* Dna2 at telomere ends. Our results suggest that Dna2 is involved in the generation of G-rich overhangs in both *taz1-d* cells and wild-type cells. We also tested the possibility that Dna2 is involved in the processing of DSB ends. However, DSB repair ability was not affected in a *dna2-C2* mutant. Although Rad50 complex is involved in the processing of both telomere ends and DSB ends, our results strongly suggest that telomere ends and DSB ends are processed by different mechanisms.

MATERIALS AND METHODS

Strain construction and growth medium. Strains used in this report are listed in Table 1. To overexpress *rad2*$^+$ gene product, pREP42X-rad2 (*ura4*$^+$) was constructed by ligation of *Bam*HI digested *rad2*$^+$, which was generated from plasmid pREP41X-rad2 (*LEU2*), with *Bam*HI digested pREP42X. pREP42X-rad2 suppressed a ts phenotype of a *dna2-C2* mutant (data not shown)(31). To tag Dna2 protein and Dna2-C2 mutant protein with Myc epitope-tag at C-terminus of the proteins, the plasmid, pFA6a-Dna2-13Myc-kanMX6 was constructed as follow. First the *dna2*$^+$ gene was amplified by PCR using the primers (Top: GCATACCCGGGTTTATAAGAAGTGGGAGAAGTTA and Bottom: GCATACCCGGGAAATTCCAGTTGAGGTAAAAT) using genomic DNA of wild-type cells (JY741) as a template. Then the *Sma*I cut PCR fragment was cloned into *Sma*I cut pFA6a-13Myc-kanMX6, resulting the plasmid, pFA6a-Dna2-13Myc-kanMX6. pFA6a-13Myc-kanMX6, which contains 13 copies of the Myc epitope and a kanMX6 marker, was provided by John R. Pringle (University of North Carolina) (8). pFA6a-Dna2-13Myc-kanMX6 was linearized with *Sph*I or *Xba*I and used for transformation of wild-type cells (JY741) or *dna2-C2* mutant cells (HK10), respectively. To tag Trt1 protein with Myc epitope-tag at the C-terminus of the proteins, the plasmid pFA6a-Trt1-13Myc-kanMX6 was constructed as follows. First, the *trt1*$^+$ gene was amplified by PCR using the primers (Top: GATATCCCCGGGACCGAACACCATACCC and Bottom: GATATCCCCGGGATCAGCTATTCTTCTATGTAAAAAT) using genomic DNA of

wild-type cells (JY741) as a template. Then the *Sma*I cut PCR fragment was cloned into *Sma*I cut pFA6a-13Myc-kanMX6, resulting the plasmid, pFA6a-Trt1-13Myc-kanMX6. pFA6a-Trt1-13Myc-kanMX6 was linearized with *Afl* II and used for transformation of *cdc25-22* cells (LSP11) and *pku70-d* cells in a *cdc25-22* background (TK001). Other double or triple mutants were constructed by genetic crosses. Cells were grown in YPAD medium (1% yeast extract, 2% polypeptone, 2% glucose, 20 μg/ml adenine) at the indicated temperature.

In-gel hybridization. In-gel hybridization analysis was performed according to the protocol previously published using a G-rich probe: 5'-GATCGGGTTACAAGGTTACG TGGTTACACG-3' and a C-rich probe: 5'-CGTGTAACCACGTAACCTTGTAACC CGATC-3' (59). One microgram of genomic DNA was digested with *Eco*RI or *Hin*dIII and separated by electrophoresis on a 0.5% agarose gel in 0.5×TAE buffer with 0.01 mg/ml ethidium bromide. Single-stranded telomeric DNA probe was labeled with [γ-^{32}P] ATP (Amersham Pharmacia Biotech) using T4 polynucleotide kinase. The gel was hybridized with 10 pmol of probe in hybridization buffer at 37°C overnight. Then the gel was washed and dried. Signals were detected using a Molecular Imager (Bio-Rad). To detect double-stranded telomeric DNA, the gel was treated with denaturing solution (0.5 M NaOH, 150 mM NaCl) for 25 min at room temperature, and then with neutralizing solution (0.5 M Tris-HCl pH 8.0 150 mM NaCl) and re-probed with the same probe by in-gel hybridization.

Measurement of telomere length. Telomere length was measured by Southern

hybridization according to the procedure described previously (20) by using an AlkPhos DirectTM kit module (Amersham Pharmacia Biotech). Briefly, chromosomal DNA, which was digested with *Apa*I and separated by electrophoresis on a 2% agarose gel, was probed with a 0.3-kb DNA fragment containing telomeric repeat sequences, which was derived from pNSU70 (52).

Chromatin immunoprecipitation. The ChIP assay described by Takahashi *et al*. was adopted with a shift modification (56). Cells grown in 100 ml of YPAD culture at the indicated temperature were fixed with formaldehyde. For immunoprecipitation, anti-Myc-Tag 9B11 antibody (Cell Signaling) and protein G-coated Dynabeads (DYNAL) were used. Immunoprecipitated DNA was extracted and suspended in TE buffer (10 mM Tris-HCl, 1 mM EDTA). The telomere DNA and the partial *ade6*$^+$ DNA were amplified by PCR with [α-^{32}P] CTP (Amersham Pharmacia Biotech) using mixed primers of telomeric DNA (Top 5'-CGGCTGACGGGTGGGGCCCAATA-3' Bottom 5'-GTGTGGAATTGAGTATGGTGAA-3') or the partial *ade6*$^+$ DNA (Top 5'-AGGTATAACGACAACAAACGTTGC -3' Bottom 5'-CAAGGCATCAGTGTTAATATGCTC-3'). PCR products were separated by electrophoresis on a 0.5% acrylamide gel (TBE buffer) and the signals were detected and quantitated using a Molecular Imager (Bio-Rad) or using a trans-illuminator and NIH image software. All experiments were repeated at least four times with similar results.

DNA damage sensitivity assay. For the spot assay, 4 μl of 10-fold dilutions of

log-phase cells ($0.5x10^7$ cells/ml) were spotted onto a YPAD (2% agar) plate or a YPAD plate containing the indicated concentration of bleomycin. For IR survival assay, logarithmically growing cells were irradiated using a ^{60}Co source at a dose rate of 100-200 Gy/hour. Irradiated cells and unirradiated cells were plated on YPAD medium plates and incubated at 25°C or 30°C for 4 days. All experiments were repeated at least twice with similar results.

RESULTS

Dna2 is required for the production of G-rich single-strand overhangs at telomere ends. It has been suggested that an unknown nuclease resects the C-rich strand at telomere ends in *taz1-d* cells (59, 61). To identify this nuclease, we first created a *taz1-d exo1-d* double mutant and a *taz1-d rad2-d* double mutant because both Exo1 and Rad2 posses 5' to 3' exonuclease activity (4, 53). However, these double mutants still contained a significant amount of G-rich overhangs (Fig. 1A, lanes 3 and 4), suggesting that the putative nuclease is neither Exo1 nor Rad2.

S. cerevisiae Dna2, which possesses nuclease activity, binds to telomere end (19) and overproduction of Dna2 leads to increased G-rich overhangs (44). Therefore, we next tested whether *S. pombe* Dna2 is required for the generation of G-rich overhangs in *taz1-d* cells. For this, we used a *dna2-C2* temperature sensitive mutant, which carries a Leu to Ser change at amino acid 1079 (31). This *dna2-C2* mutant grows normally at 25°C and at 28°C (31). We created a *taz1-d dna2-C2* double mutant and examined the overhang at both the permissive temperature (25°C) and semi-permissive temperature (30°C). The *taz1-d dna2-C2* double mutant contained a significant amount of G-rich overhangs at the permissive temperature (25°C) (Fig. 1A, lane 5). In contrast, the *taz1-d dna2-C2* double mutant lost the G-rich overhangs following a shift to the semi-permissive temperature (30°C) for 1 day (Fig. 1A, lane 7). These results indicate that Dna2 is required for the generation of G-rich overhang in *taz1-d* cells (59). We also examined the amount of G-rich overhang in *taz1-d* cells at 25°C,

and found that the signal is almost identical to that at 30°C (data not shown).

The ts phenotype of the *dna2-C2* mutant can be suppressed by overexpression of Cdc1, Cdc27, Cdc17, and Rad2 (31). As each of these gene products plays a role in the elongation or maturation of Okazaki fragments, *dna2-C2* mutant is suggested to have a defect in the Okazaki fragment elongation and maturation. If the defect in generation of G-rich overhang in *taz1-d dna2-C2* double mutant at the semi-permissive temperature is due to a defect in Okazaki fragment maturation, overexpression of Rad2 would suppress the defect in generation of G-rich overhang in *taz1 dna2-C2* double mutant. To test this possibility, we overexpressed Rad2 in *taz1-d dna2-C2* double mutant at the semi-permissive temperature and examined the overhang. Overexpression of Rad2 did not suppress the defect in generation of G-rich overhang in *taz1-d dna2-C2* double mutant, suggesting that the telomere phenotype of *dna2-C2* mutant at the semi-permissive temperature is not due to a defect in Okazaki fragment maturation (Fig. 1A, lanes 13 and 14). We also confirmed that the single-stranded DNA is present at the termini of the chromosomes in *taz1-d* cells by incubating genomic DNA in the presence of *E. coli*. Exonuclease I (Fig. 1A, lanes 11 and 12).

Although our previous work showed that the Rad50 complex, in addition to Dna2, is required for the generation of G-rich overhangs in *taz1-d* cells, a *taz1-d rad50-d pku70-d* triple mutant cells contain the overhang, suggesting that an unknown second nuclease can resect telomere ends without the assistance of Rad50 complex when both the Taz1 and Ku heterodimer are absent (59). To test the possibility that this second nuclease is also Dna2, we

examined the overhang in *taz1-d dna2-C2 pku70-d* triple mutant cells at semi-permissive temperature (30°C). The G-rich overhang was detected in the *taz1-d dna2-C2 pku70-d* triple mutant at 25°C (Fig. 1A, lane 6). However, the G-rich overhang was not detected in the *taz1-d dna2-C2 pku70-d* triple mutant at 30°C (Fig. 1A, lane 8). These results suggest that Dna2 is the second nuclease that resects telomere ends without the assistance of Rad50 complex when both the Taz1 and Ku heterodimer are absent.

In wild-type cells, the amount of G-rich overhangs increases in S phase (33). The signal corresponding to the G-rich overhang in S phase disappears by addition of *E. coli*. Exonuclease I, indicating that the single-stranded G-rich DNA detected in S phase in wild-type cells is present at the terminus of the telomere (data not shown). The next question we addressed was whether Dna2 is involved in the processing of telomere ends in S phase in wild-type cells. The mechanism of the generation of G-rich overhangs in S phase is not clear, because G-rich overhangs could be generated without nuclease activity at telomere ends that are synthesized by lagging strand DNA synthesis, simply through failure to complete lagging strand synthesis. In contrast, telomere ends synthesized by leading-strand DNA synthesis would be blunt and would require nuclease reaction to produce G-rich overhangs (17). Nonetheless, we next examined the G-rich overhangs in the *dna2-C2* mutant in S phase at the semi-permissive temperature. Wild-type cells and the *dna2-C2* mutant cells were grown at 30°C and synchronized by using an elutriator. As shown previously, the G-rich overhangs increased in S phase in wild-type cells (Figs. 1B and C). Although the G-rich overhangs also

increased in S phase in *dna2-C2* cells at the semi-permissive temperature, the signal intensity of the G-rich overhang in S phase in *dna2-C2* cells at the semi-permissive temperature was lower than that in wild-type cells (Figs. 1B and C). These results suggest that Dna2 is involved in the production of G-rich overhangs not only in *taz1-d* cells but also in wild-type cells.

Dna2 is required for telomere length maintenance. Next we examined the telomere length of the *dna2-C2* mutant at both the permissive temperature (25°C) and semi-permissive temperature (30°C). For unknown reason, the telomere lengths of wild-type cells and *rad50-d* cells at 25°C were slightly (about 10 bp) longer than those at 30°C (Fig. 2A, lanes 11-14 and Fig. 2B). In contrast, the telomere length of the *dna2-C2* mutant was significantly (about 70 bp) longer than that of the wild-type cells at 25°C (Fig. 2A, lane 2 and Fig. 2B). The telomere length of the *dna2-C2* mutant gradually decreased after the temperature shift to 30°C (Fig. 2A, lanes 3-7). The telomere length then became stable when it became similar to that of *rad50-d* mutant (Fig. 2A, lanes 7 and 9, and Fig. 2B). These results indicate that Dna2 is required for telomere length maintenance.

To test whether Rad50 and Dna2 are involved in the same pathway in telomere maintenance, we next examined the telomere length of a *rad50-d dna2-C2* double mutant at 30°C. Although the telomere length of the *rad50-d dna2-C2* double mutant was similar to that of the *dna2-C2* single mutant, they did not match completely (Fig. 3A, lanes 2 and 3). Therefore we could not conclude that Rad50 and Dna2 are involved in the same pathway in

telomere length regulation.

The deletion of any of the *rad32*$^+$, *rad50*$^+$ or *nbs1*$^+$ genes in combination with deletion of the *rad3*$^+$ gene, which is required for the response to DNA damage, causes catastrophic loss of telomeres, resulting in chromosomal end fusions (9, 16, 42). To test whether Dna2 and the Rad50 complex function in the same pathway for telomere maintenance in the absence of Rad3, we examined the telomere length of a *rad3-d dna2-C2* double mutant. Although the *rad3-d rad32-d* double mutant lost the telomere repeats completely, the *rad3-d dna2-C2* double mutant did not lose the telomere repeats (Fig. 3B, lanes 4 and 5). This result suggests that Dna2 and Rad50 have different roles in telomere maintenance in the absence of Rad3.

Since neither deletion of the *exo1*$^+$ gene in *taz1-d* cell nor deletion of the *exo1*$^+$ gene in *taz1-d rad50-d ku70-d* triple mutant cell affect the amount of G-rich overhang, Exo1 seemed to have no roles in telomere maintenance in *S. pombe* (Fig. 1A, lane 3) (59). However, we found that the telomere length of a *exo1-d dna2-C2* double mutant was shorter than that of each single mutant (Fig. 3C, lane 4). These results suggest that Exo1 plays an important role at telomere ends and that Dna2 and Exo1 function independently at telomere ends.

Dna2 binds telomeres preferentially and binding is severely impaired by temperature shift to the semi-permissive temperature. We next performed chromatin immunoprecipitation (ChIP) assays to examined whether Dna2 binds to telomere ends. We created strains in which the only wild-type copy of *dna2*$^+$ was replaced by either *dna2-myc* or

dna2-C2-myc (8). In both the wild-type cells and *dna2-C2* mutant cells, tagging of Dna2 did not affect the growth rates or the methyl methanesulfonate (MMS) and HU sensitivities (data not shown). We found that Dna2-Myc protein was bound preferentially to telomeric DNA in a ChIP assay (Figs. 4A and B). Next, we examined the telomere binding of the Dna2-C2 mutant protein. Dna2-C2-Myc mutant protein bound to telomeres at the permissive temperature. However, the telomere binding was severely impaired after shift to the semi-permissive temperature (Figs. 4A and B). The reduced telomere binding at the semi-permissive temperature was not due to reduction of protein level, because the protein level was not different in the *dna2-C2* mutant at the permissive temperature and semi-permissive temperature (Fig. 4C). Our results suggest that telomere shortening and loss of G-rich overhangs in the *dna2-C2* mutant at the semi-permissive temperature are due to loss of the telomere-binding ability of Dna2 protein.

Binding of telomerase to telomeric DNA is reduced in the *dna2-C2* mutant. We next asked whether the mutation of *dna2*$^{+}$ affects the binding of the telomerase catalytic subunit, Trt1, to telomeric DNA. As shown in Figures 5A and B, Myc-tagged Trt1 bound to telomeric DNA. In contrast, the binding of Trt1 to telomeric DNA was reduced in the *dna2-C2* mutant at the semi-permissive temperature (Figs. 5A and B). The protein expression level of Trt1-myc was not affected in the *dna2-C2* mutant, indicating that the reduced binding was not due to a reduced protein level (data not shown). As *dna2-C2* mutant has short telomeres, the reduced telomere binding of telomerase might have been due to telomere

shortening. To test this possibility, we examined the telomere binding of Trt1 in *pku70-d* cells, which have short telomeres. The binding of Trt1 to telomeric DNA was not affected in *pku70-d* cells, suggesting that the reduced telomere binding of Trt1 in the *dna2-C2* mutant is not due to reduced telomere length (Fig. 5C).

DSB repair ability is not affected in the *dna2-C2* mutant. Our results suggest that Dna2 is involved in the production of G-rich overhangs at telomere ends. The next question is whether Dna2 is involved in the processing of DSB ends. To address this, we examined the sensitivity of the *dna2-C2* mutant to bleomycin and γ-rays at 25°C and 30°C. The sensitivities to bleomycin and γ-rays at 30°C were not affected by the mutation of $dna2^{+}$ (Fig. 6). These results suggest that the DBS repair ability, including the ability to process DSB ends, is not affected by the *dna2-C2* mutation.

DISCUSSION

Dna2 is required for generation of G-rich overhangs in *taz1-d* cells. We found that a *dna2-C2 taz1-d* double mutant lost the G-rich overhang at the semi-permissive temperature (30°C), indicating that Dna2 is required for generation of G-rich overhangs in *taz1-d* cells (Fig. 1A). This was not due to a defect in Okazaki fragment maturation, because a *rad2-d taz1-d* double mutant did not lose the G-rich overhangs (Fig. 1A). How does Dna2 contribute to generate the G-rich overhangs in *taz1-d* cells? *S. cerevisiae* Dna2 possess endonuclease activity and can remove 5' flap DNA likely to be generated during Okazaki fragment processing in vitro (6). We have also found that purified *S. pombe* Dna2 has nuclease activity (data not shown). Therefore, we propose a model in which Dna2 is required for degradation of the C-rich strand in *taz1-d* cells, similar to the mechanism of removal of the 5' flap DNA during Okazaki fragment processing (Fig. 7A). In this model, telomere ends would be unwound by the Rad50 complex and/or unknown helicase. Then, Dna2 would remove 5' flap DNA by using its endonuclease activity. *S. cerevisiae* Dna2 possesses helicase activity. In contrast, purified *S. pombe* Dna2 lacks any detectable ATPase activity, suggesting that *S. pombe* Dna2 has no helicase activity (7, 14, 57). However, it could be possible that helicase domain of Dna2 might have some role in DNA unwinding, because the human Rad50 complex has DNA unwinding activity in the absence of ATP (46). Therefore, we do not exclude the possibility that the DNA unwinding activity of Dna2, but not a nuclease activity, is required for the processing of telomeric DNA.

Another possible explanation for the lack of G-rich overhang in the *taz1-d dna2-C2* double mutant at the semi-permissive temperature is that Dna2 protects G-rich overhangs from degradation. If this were true, G-rich overhangs would not be detected in S phase in the *dna2-C2* mutant at the semi-permissive temperature. However, the G-rich overhang was still detected in S phase in the *dna2-C2* mutant (Fig. 1B and C), making this explanation is unlikely.

Consistent with our two-step model, the binding of Dna2-Myc protein to the telomeres in a ChIP assay was not affected in the *rad32-d* mutant (data not shown). Moreover, Rad32-Myc protein bound to telomeric DNA in a *dna2-C2* mutant background at both 25°C and 30°C in a ChIP assay (data not shown). These results indicate that Dna2 and the Rad50 complex bind to telomere independently. We also tested the interaction between Dna2 and the Rad50 complex by co-immunoprecipitation experiments and found that Dna2-Myc protein was not co-immunoprecipitated with Rad50-TAP protein, suggesting that Dna2 does not stably interact with the Rad50 complex *in vivo* (data not shown). Although we assume that the nuclease activity of Dna2 is involved in telomere processing, it remains unclear whether Dna2-C2 mutant protein has defect in nuclease activity at semi-permissive temperature. Further biochemical studies are required to confirm our model.

As a *taz1-d rad50-d pku70-d* triple mutant possesses the G-rich overhangs, the existence of a second nuclease that resects telomere ends without assistance from the Rad50 complex in the absence of Taz1 and Ku heterodimer has been suggested (Fig. 7B) (59). We

found that a *taz1-d dna2-C2 pku70-d* triple mutant did not have the G-rich overhangs at the semi-permissive temperature, suggesting that this second nuclease is also Dna2 (Fig. 1A and Fig. 7B). These results suggest that the Rad50 complex allows Dna2 to resect telomere ends in the presence of Ku heterodimer, but in the absence of Ku heterodimer, Dna2 can resect telomere ends without assistance from the Rad50 complex (Fig. 7B). How does Rad50 complex allow Dna2 to resect telomere ends in the presence of Ku heterodimer? In our model, telomere ends must be unwound by a helicase activity. As Ku heterodimer binds and protects DNA ends from enzymes activity such as nucleases, Ku might inhibit DNA unwinding at telomere ends. In that case, the Rad50 complex might be required for DNA unwinding in the presence of Ku heterodimer.

Mutation in *dna2*$^{+}$ affects the generation of G-rich overhangs in S phase in wild-type cells. Although the above model was substantiated based on the study using *taz1-d* backdround, this model might be applicable to the case in the generation of G-rich overhang in S phase in wild-type cells, because Taz1 inhibits telomerase activity and Taz1 might be detached from telomeric DNA or inactivated in S phase to allow telomerase to access telomere ends. To test this possibility, we examined the effect of *dna2-C2* mutation on the G-rich overhang in S phase in wild-type background. In wild-type cells, the intensity of the signal corresponding to the G-rich overhang increased 16.50% in S phase compared to G2 phase. In contrast, in the *dna2-C2* mutant, the signal intensity increased only 8.36% in S phase compared to G2 phase at the semi-permissive temperature (Figs. 1B and C). We assume

that this reduction in G-rich overhangs in S phase in the *dna2-C2* mutant can be attributed to the defect in the degradation of the C-rich strand by Dna2. Although G-rich overhangs were still detected in the *dna2-C2* mutant in S phase, these G-rich overhangs could have been produced without nuclease activity at telomere ends that were synthesized by lagging strand DNA synthesis. Therefore we assume that the G-rich overhang detected in the *dna2-C2* mutant in S phase is produced without nuclease activity. At this time, however, it is impossible to distinguish the telomere ends synthesized by leading strand DNA synthesis from those generated by lagging strand. Further studies will be required to elucidate the detailed roles of Dna2 at telomere ends in S phase.

We found that the telomere length of a *dna2-C2 exo1-d* double mutant was shorter than that of each single mutant at 30°C (Fig. 3C). These results indicate that Dna2 and Exo1 function independently at telomere ends. In *S. cerevisiae*, Exo1 is required for the production of G-rich overhangs in a *yku70* mutant (37). Similarly, *S. pombe* Exo1 might be able to produce the G-rich overhangs in the *dna2-C2* mutant via its exonuclease activity. These facts further support our model that Dna2 is required for the production of the G-rich overhangs in wild-type cells.

The role of Dna2 on the recruitment of telomerase to telomere DNA. We found that the binding of Trt1 was reduced in the *dna2-C2* mutant at semi-permissive temperature (Fig. 5). Our results suggest that Dna2 is involved in the production of G-rich overhangs in wild-type cells (Fig. 1B and C). Telomerase binds to G-rich overhangs to elongate telomeric

DNA. These facts suggest that the reduced telomere binding of telomerase in the *dna2-C2* mutant is due to the reduced G-rich overhangs. If Trt1 binding to telomere depends on the length of the single-stranded overhang, Trt1 might bind to telomere more tightly in *pku70-d* cells than in wild-type cells, because *pku70-d* cells have longer overhangs than wild-type cells (33). However, the telomere binding of telomerase did not increase in *pku70-d* cells. The possible explanation for this is that telomerase binding might be saturated in the wild-type cells and hence longer overhangs in *pku70-d* cells might not lead to increased Trt1 binding.

The other explanation for the reduced telomere binding of telomerase in the *dna2-C2* mutant is that Dna2 is required for the recruitment of telomerase through protein-protein interaction. *S. cerevisiae* Dna2 binds to Replication protein A (RPA). RPA also binds to telomere DNA in both *S. pombe* and *S. cerevisiae* (43, 50). Moreover, *S. cerevisiae* RPA is required for loading Est1p onto telomeres during S phase (43, 50). These facts imply that *S. pombe* Dna2 might be involved in the loading of telomerase complex to telomere.

Telomere shortening of *dna2-C2* mutant cells at the semi-permissive temperature can be explained by the defect in telomere end processing and/or insufficient recruitment of telomerase to telomeric DNA. However, these *dna2-C2* mutant cells had longer telomeres than wild-type cells at the permissive temperature (Figs. 2A and B). These results suggest that the *dna2-C2* mutant has opposite defects in telomere length regulation at these two different temperatures. In *S. cerevisiae*, mutations in *POL1* and other replication proteins, including

DNA2, also cause telomere elongation (1, 15, 22, 26). It has been suggested that this elongation is due to defects in the coordination of DNA polymerase alpha with telomerase activity (2, 18, 47, 48). Similarly, at the permissive temperature, *S. pombe dna2-C2* mutant might have a defect in the coordination of DNA polymerase alpha with telomerase activity, which might allow uncontrolled telomere elongation.

Defect in telomere end processing is not related to the defect in telomere maintenance in the absence of Rad3. Both Dna2 and Rad50 complex are required for the generation of G-rich overhangs in *taz1-d* cells. (Figs. 2A). This fact suggests that Dna2 and Rad50 are epistatic in telomere end resection. Although *rad3-d rad50-d* double mutant and *rad3-d rad32-d* double mutant lose telomere DNA completely (Fig. 3B) (42), the *rad3-d dna2-C2* double mutant did not lose telomere DNA at the semi-permissive temperature (Fig. 3B). These results indicate that Dna2 and Rad50 are not epistatic in telomere maintenance in the absence of Rad3. It has been suggested that Tel1 and Rad50 function in the same pathway for telomere maintenance in the absence of Rad3 (39, 40, 42). Therefore, we tested whether Tel1 is required for generation of G-rich overhangs in *taz1-d* cells. However, we found that deletion of $tel1^{+}$ in the *taz1-d* mutant did not affect the G-rich overhang (data not shown). This result indicates that Tel1 is not epistatic to Rad50 in the generation of G-rich overhang in *taz1-d* cells. Our results allow us to dissect the telomere end resection in *taz1-d* cells and telomere maintenance in the absence of Rad3. Rad50 is required for both processes, whereas Dna2 is involved only in the former and Tel1 only in the latter.

The role of Dna2 on DNA repair. *dna2-C2* mutant is MMS and HU sensitive, suggesting that *dna2*$^{+}$ is involved in repair of DNA damage generated by alkylating agents (31). Surprisingly, *dna2-C2* mutant was not γ-ray sensitive, suggesting that *dna2*$^{+}$ is not involved in repair of DNA damage generated by γ-ray. MMS stalls replication fork and is thought to collapse replication fork in *S. pombe* (28, 59). In contrast, γ-ray causes DNA double-strand breaks mostly in G2 phase and repaired in G2 phase. These facts suggest that Dna2 is specifically required for DNA damage generated at stalled or collapsed replication fork. Similar to the *dna2-C2* mutant, *S. pombe mus81-d* cells are MMS sensitive, but not γ-ray sensitive. Mus81 is also suggested to be involved in processing of collapsed replication fork (10, 24).

Difference between DSB ends and telomere ends. Although the Rad50 complex is involved in the processing of both telomere ends and DSB ends, our results revealed that DSB ends and telomere ends are processed differently. Our results suggest that Dna2 is involved in the processing of telomere ends. However, the DSB repair ability (probably including the DSB end processing ability) was normal in the *dna2-C2* mutant at the semi-permissive temperature, suggesting that Dna2 is not involved in the processing of DSB ends (Fig. 6)(59). Consistent with this data, *S. cerevisiae dna2* mutants that are sensitive to X-rays are not defective in mitotic recombination, suggesting that *S. cerevisiae* Dna2 is not involved in the processing of DSB ends (11). The mechanism of processing of DSB ends is not fully understood. It is clear that the Rad50 complex is involved in this process. However

the importance of the nuclease domain in Rad32 remains unclear. The *S. pombe rad32-D25A* mutant is DNA damage sensitive, but the complex formed between Rad32 and Rad50 is unstable in the *rad32-D25A* mutant (59). Therefore, the DNA damage sensitivity of the *rad32-D25A* mutant might be due to defective formation of the complex between Rad32 and Rad50. In *S. cerevisiae*, nuclease-deficient *mre11* mutant is not as DNA damage sensitive as *mre11* null mutant. Based on these and other data, the existence of an unknown nuclease that resects DSB ends has been suggested (35). Although our results suggest that Dna2 is not involved in the processing of DSB ends, we have not excluded the possibility that another *dna2* mutant alleles might have a defect in DSB end processing. Isolation of additional *dna2* mutant alleles will provide useful information for elucidating the roles of Dna2 in telomere maintenance and other aspects of DNA metabolism.

Finally, our results and previous results indicate that *S. pombe* and *S. cerevisiae* Dna2 play important roles at telomere ends (19). Dna2 is conserved from yeast to higher eukaryote and thus the function of Dna2 at telomere DNA might be conserved in higher eukaryotes.

ACKNOWLEDGEMENTS

We are grateful to Judith Campbell for suggesting that Dna2 might be involved in the processing of telomere ends. We thank Hiroyuki Araki for help with the elutriation, Takeshi Saito, Shinji Yasuhira and Hiroshi Utsumi for help with the γ-ray irradiation, and Hiroshi Iwasaki and Akira Matsuura for providing strains, and John R. Pringle for providing plasmids. We also thank all the members of our laboratory for their valuable discussions and help for revision and Julia Cooper for allowing Kazunori Tomota to do some experiments for revision at her Lab in Cancer Research UK. This work was supported by Grants-in-Aid for Scientific Research on Priority Areas from the Ministry of Education, Science, Sports and Culture of Japan to Masaru Ueno, and by a grant from the Yokohama City Collaboration of Regional Entities for the Advancement of Technological Excellence, JST, to Masaru Ueno. This work was supported by NIB Cooperative Research Program (2004-8).

REFERENCES

1. **Adams, A. K., and C. Holm.** 1996. Specific DNA replication mutations affect telomere length in *Saccharomyces cerevisiae*. Mol. Cell. Biol. **16:**4614-20.

2. **Adams Martin, A., I. Dionne, R. J. Wellinger, and C. Holm.** 2000. The function of DNA polymerase alpha at telomeric G tails is important for telomere homeostasis. Mol. Cell. Biol. **20:**786-96.

3. **Alfa, C., P. Fantes, J. Hyams, M. McLeod, and E. Warbrick.** 1993. Experiments with Fission Yeast. Cold Spring Harbor Laboratory Press.

4. **Alleva, J. L., and P. W. Doetsch.** 1998. Characterization of *Schizosaccharomyces pombe* Rad2 protein, a FEN-1 homolog. Nucleic Acids Res. **26:**3645-50.

5. **Ayyagari, R., X. V. Gomes, D. A. Gordenin, and P. M. Burgers.** 2003. Okazaki fragment maturation in yeast. I. Distribution of functions between Fen1 and Dna2. J. Biol. Chem. **278:**1618-25.

6. **Bae, S. H., K. H. Bae, J. A. Kim, and Y. S. Seo.** 2001. RPA governs endonuclease switching during processing of Okazaki fragments in eukaryotes. Nature **412:**456-61.

7. **Bae, S. H., J. A. Kim, E. Choi, K. H. Lee, H. Y. Kang, H. D. Kim, J. H. Kim, K. H. Bae, Y. Cho, C. Park, and Y. S. Seo.** 2001. Tripartite structure of *Saccharomyces cerevisiae* Dna2 helicase/endonuclease. Nucleic Acids Res. **29:**3069-79.

8. **Bahler, J., J. Q. Wu, M. S. Longtine, N. G. Shah, A. McKenzie, 3rd, A. B. Steever, A. Wach, P. Philippsen, and J. R. Pringle.** 1998. Heterologous modules for efficient

and versatile PCR-based gene targeting in *Schizosaccharomyces pombe*. Yeast **14:**943-51.

9. **Bentley, N. J., D. A. Holtzman, G. Flaggs, K. S. Keegan, A. DeMaggio, J. C. Ford, M. Hoekstra, and A. M. Carr.** 1996. The *Schizosaccharomyces pombe rad3* checkpoint gene. EMBO J. **15:**6641-51.

10. **Boddy, M. N., A. Lopez-Girona, P. Shanahan, H. Interthal, W. D. Heyer, and P. Russell.** 2000. Damage tolerance protein Mus81 associates with the FHA1 domain of checkpoint kinase Cds1. Mol Cell Biol **20:**8758-66.

11. **Budd, M. E., and J. L. Campbell.** 2000. The pattern of sensitivity of yeast dna2 mutants to DNA damaging agents suggests a role in DSB and postreplication repair pathways. Mutat. Res. **459:**173-86.

12. **Budd, M. E., and J. L. Campbell.** 1995. A yeast gene required for DNA replication encodes a protein with homology to DNA helicases. Proc. Natl. Acad. Sci. U. S. A. **92:**7642-6.

13. **Budd, M. E., and J. L. Campbell.** 1997. A yeast replicative helicase, Dna2 helicase, interacts with yeast FEN-1 nuclease in carrying out its essential function. Mol. Cell. Biol. **17:**2136-42.

14. **Budd, M. E., W. C. Choe, and J. L. Campbell.** 1995. *DNA2* encodes a DNA helicase essential for replication of eukaryotic chromosomes. J. Biol. Chem. **270:**26766-9.

15. **Carson, M. J., and L. Hartwell.** 1985. *CDC17*: an essential gene that prevents telomere elongation in yeast. Cell **42:**249-57.

16. **Chahwan, C., T. M. Nakamura, S. Sivakumar, P. Russell, and N. Rhind.** 2003. The fission yeast Rad32 (Mre11)-Rad50-Nbs1 complex is required for the S-phase DNA damage checkpoint. Mol. Cell. Biol. **23:**6564-73.

17. **Chakhparonian, M., and R. J. Wellinger.** 2003. Telomere maintenance and DNA replication: how closely are these two connected? Trends Genet **19:**439-46.

18. **Chandra, A., T. R. Hughes, C. I. Nugent, and V. Lundblad.** 2001. Cdc13 both positively and negatively regulates telomere replication. Genes Dev. **15:**404-14.

19. **Choe, W., M. Budd, O. Imamura, L. Hoopes, and J. L. Campbell.** 2002. Dynamic localization of an Okazaki fragment processing protein suggests a novel role in telomere replication. Mol. Cell. Biol. **22:**4202-17.

20. **Cooper, J. P., E. R. Nimmo, R. C. Allshire, and T. R. Cech.** 1997. Regulation of telomere length and function by a Myb-domain protein in fission yeast. Nature **385:**744-7.

21. **D'Amours, D., and S. P. Jackson.** 2002. The Mre11 complex: at the crossroads of DNA repair and checkpoint signalling. Nat. Rev. Mol. Cell. Biol. **3:**317-27.

22. **Dahlen, M., P. Sunnerhagen, and T. S. Wang.** 2003. Replication proteins influence the maintenance of telomere length and telomerase protein stability. Mol. Cell. Biol. **23:**3031-42.

23. **Dionne, I., and R. J. Wellinger.** 1996. Cell cycle-regulated generation of single-stranded G-rich DNA in the absence of telomerase. Proc. Natl. Acad. Sci. U. S. A. **93:**13902-7.

24. **Doe, C. L., J. S. Ahn, J. Dixon, and M. C. Whitby.** 2002. Mus81-Eme1 and Rqh1 involvement in processing stalled and collapsed replication forks. J. Biol. Chem. **277:**32753-9.

25. **Ferreira, M. G., K. M. Miller, and J. P. Cooper.** 2004. Indecent exposure: when telomeres become uncapped. Mol. Cell **13:**7-18.

26. **Formosa, T., and T. Nittis.** 1999. Dna2 mutants reveal interactions with Dna polymerase alpha and Ctf4, a Pol alpha accessory factor, and show that full Dna2 helicase activity is not essential for growth. Genetics **151:**1459-70.

27. **Furuse, M., Y. Nagase, H. Tsubouchi, K. Murakami-Murofushi, T. Shibata, and K. Ohta.** 1998. Distinct roles of two separable *in vitro* activities of yeast Mre11 in mitotic and meiotic recombination. EMBO J. **17:**6412-25.

28. **Hartsuiker, E., E. Vaessen, A. M. Carr, and J. Kohli.** 2001. Fission yeast Rad50 stimulates sister chromatid recombination and links cohesion with repair. EMBO J. **20:**6660-71.

29. **Hiraoka, Y., E. Henderson, and E. H. Blackburn.** 1998. Not so peculiar: fission yeast telomere repeats. Trends Biochem. Sci. **23:**126.

30. **Jin, Y. H., R. Ayyagari, M. A. Resnick, D. A. Gordenin, and P. M. Burgers.** 2003.

Okazaki fragment maturation in yeast. II. Cooperation between the polymerase and 3'-5'-exonuclease activities of Pol delta in the creation of a ligatable nick. J. Biol. Chem. **278:**1626-33.

31. **Kang, H. Y., E. Choi, S. H. Bae, K. H. Lee, B. S. Gim, H. D. Kim, C. Park, S. A. MacNeill, and Y. S. Seo.** 2000. Genetic analyses of *Schizosaccharomyces pombe dna2*$^{+}$ reveal that dna2 plays an essential role in Okazaki fragment metabolism. Genetics **155:**1055-67.

32. **Kao, H. I., J. Veeraraghavan, P. Polaczek, J. L. Campbell, and R. A. Bambara.** 2004. On the roles of *Saccharomyces cerevisiae* Dna2p and FEN1 in Okazaki fragment processing. J. Biol. Chem.

33. **Kibe, T., K. Tomita, A. Matsuura, D. Izawa, T. Kodaira, T. Ushimaru, M. Uritani, and M. Ueno.** 2003. Fission yeast Rhp51 is required for the maintenance of telomere structure in the absence of the Ku heterodimer. Nucleic Acids Res. **31:**5054-63.

34. **Kuo, C., H. Nuang, and J. L. Campbell.** 1983. Isolation of yeast DNA replication mutants in permeabilized cells. Proc. Natl. Acad. Sci. U. S. A. **80:**6465-9.

35. **Lee, S. E., D. A. Bressan, J. H. Petrini, and J. E. Haber.** 2002. Complementation between N-terminal *Saccharomyces cerevisiae mre11* alleles in DNA repair and telomere length maintenance. DNA Repair (Amst) **1:**27-40.

36. **Makarov, V. L., Y. Hirose, and J. P. Langmore.** 1997. Long G tails at both ends of

human chromosomes suggest a C strand degradation mechanism for telomere shortening. Cell **88:**657-66.

37. **Maringele, L., and D. Lydall.** 2002. EXO1-dependent single-stranded DNA at telomeres activates subsets of DNA damage and spindle checkpoint pathways in budding yeast *yku70*Delta mutants. Genes Dev. **16:**1919-33.

38. **Moreau, S., J. R. Ferguson, and L. S. Symington.** 1999. The nuclease activity of Mre11 is required for meiosis but not for mating type switching, end joining, or telomere maintenance. Mol. Cell. Biol. **19:**556-66.

39. **Naito, T., A. Matsuura, and F. Ishikawa.** 1998. Circular chromosome formation in a fission yeast mutant defective in two ATM homologues. Nat. Genet. **20:**203-6.

40. **Nakada, D., K. Matsumoto, and K. Sugimoto.** 2003. ATM-related Tel1 associates with double-strand breaks through an Xrs2-dependent mechanism. Genes Dev. **17:**1957-62.

41. **Nakamura, T. M., G. B. Morin, K. B. Chapman, S. L. Weinrich, W. H. Andrews, J. Lingner, C. B. Harley, and T. R. Cech.** 1997. Telomerase catalytic subunit homologs from fission yeast and human. Science **277:**955-9.

42. **Nakamura, T. M., B. A. Moser, and P. Russell.** 2002. Telomere binding of checkpoint sensor and DNA repair proteins contributes to maintenance of functional fission yeast telomeres. Genetics **161:**1437-52.

43. **Ono, Y., K. Tomita, A. Matsuura, T. Nakagawa, H. Masukata, M. Uritani, T.**

Ushimaru, and M. Ueno. 2003. A novel allele of fission yeast *rad11* that causes defects in DNA repair and telomere length regulation. Nucleic Acids Res. **31:**7141-9.

44. **Parenteau, J., and R. J. Wellinger.** 1999. Accumulation of single-stranded DNA and destabilization of telomeric repeats in yeast mutant strains carrying a deletion of *RAD27*. Mol. Cell. Biol. **19:**4143-52.

45. **Paull, T. T., and M. Gellert.** 1998. The 3' to 5' exonuclease activity of Mre 11 facilitates repair of DNA double-strand breaks. Mol. Cell. **1:**969-79.

46. **Paull, T. T., and M. Gellert.** 1999. Nbs1 potentiates ATP-driven DNA unwinding and endonuclease cleavage by the Mre11/Rad50 complex. Genes Dev. **13:**1276-88.

47. **Qi, H., and V. A. Zakian.** 2000. The *Saccharomyces* telomere-binding protein Cdc13p interacts with both the catalytic subunit of DNA polymerase alpha and the telomerase-associated Est1 protein. Genes Dev. **14:**1777-88.

48. **Ray, S., Z. Karamysheva, L. Wang, D. E. Shippen, and C. M. Price.** 2002. Interactions between telomerase and primase physically link the telomere and chromosome replication machinery. Mol. Cell. Biol. **22:**5859-68.

49. **Raymond, W. E., and N. Kleckner.** 1993. RAD50 protein of *S.cerevisiae* exhibits ATP-dependent DNA binding. Nucleic Acids Res. **21:**3851-6.

50. **Schramke, V., P. Luciano, V. Brevet, S. Guillot, Y. Corda, M. P. Longhese, E. Gilson, and V. Geli.** 2004. RPA regulates telomerase action by providing Est1p access to chromosome ends. Nat. Genet. **36:**46-54.

51. **Stewart, S. A., I. Ben-Porath, V. J. Carey, B. F. O'Connor, W. C. Hahn, and R. A. Weinberg.** 2003. Erosion of the telomeric single-strand overhang at replicative senescence. Nat. Genet. **33:**492-6.

52. **Sugawara, N.** 1988. DNA Sequences at the Telomeres of the Fission Yeast *S. pombe*. Ph. D. Thesis. Cambrige, MA: Harvard University.

53. **Szankasi, P., and G. R. Smith.** 1995. A role for exonuclease I from *S. pombe* in mutation avoidance and mismatch correction. Science **267:**1166-9.

54. **Taggart, A. K., S. C. Teng, and V. A. Zakian.** 2002. Est1p as a cell cycle-regulated activator of telomere-bound telomerase. Science **297:**1023-6.

55. **Taggart, A. K., and V. A. Zakian.** 2003. Telomerase: what are the Est proteins doing? Curr. Opin. Cell. Biol. **15:**275-80.

56. **Takahashi, K., S. Saitoh, and M. Yanagida.** 2000. Application of the chromatin immunoprecipitation method to identify in vivo protein-DNA associations in fission yeast. Sci. STKE. **2000:**PL1.

57. **Tanaka, H., G. H. Ryu, Y. S. Seo, K. Tanaka, H. Okayama, S. A. MacNeill, and Y. Yuasa.** 2002. The fission yeast *pfh1*$^{+}$ gene encodes an essential 5' to 3' DNA helicase required for the completion of S-phase. Nucleic Acids Res. **30:**4728-39.

58. **Tauchi, H., S. Matsuura, J. Kobayashi, S. Sakamoto, and K. Komatsu.** 2002. Nijmegen breakage syndrome gene, NBS1, and molecular links to factors for genome stability. Oncogene **21:**8967-80.

59. **Tomita, K., A. Matsuura, T. Caspari, A. M. Carr, Y. Akamatsu, H. Iwasaki, K. I. Mizuno, K. Ohta, M. Uritani, T. Ushimaru, K. Yoshinaga, and M. Ueno.** 2003. Competition between the Rad50 Complex and the Ku Heterodimer Reveals a Role for Exo1 in Processing Double-Strand Breaks but Not Telomeres. Mol. Cell. Biol. **23:**5186-5197.

60. **Trujillo, K. M., S. S. Yuan, E. Y. Lee, and P. Sung.** 1998. Nuclease activities in a complex of human recombination and DNA repair factors Rad50, Mre11, and p95. J. Biol. Chem. **273:**21447-50.

61. **Ueno, M., T. Nakazaki, Y. Akamatsu, K. Watanabe, K. Tomita, H. D. Lindsay, H. Shinagawa, and H. Iwasaki.** 2003. Molecular Characterization of the *Schizosaccharomyces pombe nbs1*$^{+}$ Gene Involved in DNA Repair and Telomere Maintenance. Mol. Cell. Biol. **23:**6553-6563.

62. **Usui, T., T. Ohta, H. Oshiumi, J. Tomizawa, H. Ogawa, and T. Ogawa.** 1998. Complex formation and functional versatility of Mre11 of budding yeast in recombination. Cell **95:**705-16.

63. **Wellinger, R. J., A. J. Wolf, and V. A. Zakian.** 1993. *Saccharomyces* telomeres acquire single-strand TG_{1-3} tails late in S phase. Cell **72:**51-60.

FIGURE LEGENDS

Fig. 1. Dna2 is involved in the generation of G-rich overhangs. (**A**) The single-stranded overhangs in various nuclease mutants in a *taz1-d* background were detected by in-gel hybridization. Lanes 1 and 11, *taz1-d* (KT110) at 30°C. Lane 2, *rad50-d taz1-d* (KT021) at 30°C. Lane 3, *exo1-d taz1-d* (KT01g) at 30°C. Lane 4, *taz1-d rad2-d* . (KT11f) at 30°C. Lane 5, *taz1-d dna2-C2* (KT010n) at 25°C. Lane 6, *taz1-d dna2-C2 pku70-d* (KT1105n) at 25°C. Lane 7, *taz1-d dna2-C2* (KT010n) at 30°C. Lane 8, *taz1-d dna2-C2 pku70-d* (KT1105n) at 30°C. Lane 9, dsDNA control. Lane 10, ss DNA control. Lane 12, *taz1-d* (KT110) at 30°C with *E. coli*. Exonuclease I. Lane 13, *taz1-d dna2-C2* (KT010n) with pREP42X (empty vector) at 30°C. Lane 14, *taz1-d dna2-C2* (KT010n) with pREP42X-rad2 (overexpression of Rad2) at 30°C. A plasmid containing the telomere-repeat sequence derived from pNSU70 was used as a dsDNA and ssDNA control (59). Genomic DNA was digested with *Eco*RI and separated by electrophoresis. Then the gel was dried and hybridized with a ^{32}P-labeled C-rich (C-probe, top panel) or G-rich (G-probe, bottom panel) probe. To detect the double-stranded telomere DNAs, the gel was treated with denaturant and reprobed with the C-rich probe (Denature, middle panel). Telomeres are indicated by arrows. (**B**) The single-stranded overhang in G2 and S phase in wild-type cells and *dna2-C2* mutant cells was detected by in-gel hybridization at a semi-permissive temperature (30°C). Lane 1, wild-type cells (JY741) in G2 phase. Lane 2, *dna2-C2* cells (HK10) in G2 phase. Lane 3, wild-type cells (JY741) in S phase. Lane 4, *dna2-C2* cells (HK10) in S phase. Lane 5, dsDNA control. Lane 6, ssDNA

control. Cells were cultured at 30°C. Then cells in G2 phase and S phase (when the septation index became maximal) were collected from logarithmically growing cells by using an elutriator (3). The septation indexes of wild-type cells and *dna2-C2* cells were 34.2% and 33.6%, respectively. Genomic DNA was digested with *Hin*dIII and the single-stranded overhang was detected as shown in Fig. 1A. Telomeres are indicated by arrows. (**C**) Quantitation of the band intensity of the in-gel hybridization assay shown in Fig. 1B. The band intensity was quantitated using a Molecular Imager (Bio-Rad). The signal intensity was calculated as follows. First the non-specific signal detected with the G-rich probe (G-probe) was subtracted from the signal corresponding to the G-rich overhang (C-probe) and from the double-strand telomere DNA signal, ([C-probe]-[G-probe]) and ([Denature]-[G-probe]), respectively. Then the signal ([C-probe]-[G-probe]) was divided by ([Denature]-[G-probe]) to adjust for the DNA concentration. Standard deviations determined from two independent experiments are shown by error bars.

Fig. 2. Dna2 is required for the telomere length regulation. (**A**) The telomere length of the *dna2-C2* mutant was analyzed by Southern hybridization analysis at the permissive (25°C) and semi-permissive temperature (30°C). Lanes 1, 10, and 11 wild-type cells at 30°C (JY741). Lane 2, *dna2-C2* mutant at 25°C (HK10). Lanes 3 to 7, *dna2-C2* mutant incubated at 30°C (HK10) for the indicated number of days. Lane 8, *dna2-C2* mutant incubated at 30°C for 25 days in an independent experiment (HK10). Incubation length is indicated above the figure.

Lanes 9 and 13, *rad50-d* at 30°C (KT120). Lane 12, wild-type cells at 25°C (JY741). Lane 14, *rad50-d* at 25°C (KT120). (**B**) Time course of the change of telomere length in *dna2-C2* mutant after temperature shift to the semi-permissive temperature (30°C). The data shown in Fig. 2A were plotted.

Fig. 3. Epistasis analysis between *dna2-C2* mutant and *rad50-d* cells (A), *rad3-d* cells (B) or *exo1-d* cells (C) for telomere maintenance at 30°C. (**A**) Telomere length of the *rad50-d dna2-C2* double mutant is slightly shorter than that of the *dna2-C2* single mutant. Lane 1, wild-type cells (JY741). Lane 2, *dna2-C2* mutant (HK10). Lane 3, *rad50-d dna2-C2* (KT120n). (**B**) Dna2 is not required for telomere maintenance in the absence of Rad3. Lane 1, wild-type cells (JY741). Lane 2, *dna2-C2* mutant (HK10). Lane 3, *rad3-d* (Rad3D). Lane 4, *rad3-d dna2-C2* (KT004n). Lane 5, *rad3-d rad32-d* (KT146). (**C**) Dna2 and Exo1 function independently for telomere length regulation. Lane 1, wild-type cells (JY741). Lane 2, *dna2-C2* mutant (HK10). Lane 3, *exo1-d* (KT00g). Lane 4, *exo1-d dna2-C2* (KT10gn). Telomere length was studied as in Fig. 2A. Because of the phenotypic lag, cells were incubated for 10 days after the temperature shift to the semi-permissive temperature (30°C). Peaks and distributions of the telomeric DNA-derived bands analyzed using NIH image 1.62 software are shown below. Telomere peaks are indicated by lines.

Fig. 4. Binding of Dna2-C2 mutant protein to telomere DNA is severely impaired by a temperature shift to the semi-permissive temperature. (**A**) ChIP assay of Dna2 protein. Untagged wild-type control cells (JY741), *dna2-myc* (KTtnM) cells and *dna2-C2-myc* (KTtnMM1) cells were cultured at the indicated temperature. PCRs were performed on whole-cell extract (Input) and on chromatin immunoprecipitates (IP with anti-Myc) using primers to amplify telomere DNA (telomere) and primers to amplify DNA from the *ade6*$^{+}$ gene (*ade6*). The relative fold enrichment of precipitated telomere DNA is shown underneath each lane. Ratios of telomere signals to *ade6* signals were used to calculate relative precipitated fold enrichment. (**B**) The relative precipitated fold enrichment determined in the ChIP assay shown in Fig. 4A was plotted. Standard deviations determined from four independent experiments are shown by error bars. As a control, the ChIP assay was performed without cross-linking (w/o crosslinking). (**C**) Protein expression level is not affected in the *dna2-C2* mutant at the permissive temperature versus semi-permissive temperature. Dna2-Myc protein from *dna2-myc* cells (KTtnM) cells and Dna2-C2-Myc protein from *dna2-C2-myc* cells (KTtnMM1) were detected by Western blotting with anti-Myc 9B11 antibody (Cell Signaling). As a control, Cdc2 was also detected with anti-Cdc2 antibody (PSTAIRE). The relative amount of Dna2 or Dna2-C2 is shown underneath each lane. Ratios of Dna2 or Dna2-C2 signals to Cdc2 signals were calculated to express the relative amount of Dna2 or Dna2-C2.

Fig. 5. Telomere binding of Trt1 is affected in *dna2-C2* mutant at 30°C. (**A**) ChIP assay of Trt1 protein in *dna2-C2* mutant. Untagged wild-type control cells (JY741), *trt1-myc* (TKt7M) cells and *trt1-myc dna2-C2* (KT000n-t7M) cells were cultured at 30°C. PCRs were performed as in Fig. 4A. (**B**) The relative precipitated fold enrichment determined in the ChIP assay shown in Fig. 5A was plotted. Standard deviations determined from four independent experiments are shown by error bars. As a control, the ChIP assay was performed without cross-linking (w/o crosslinking). (**C**) ChIP assay of Trt1 protein in *pku70-d* cells. Untagged wild-type control cells (LSP11), *trt1-myc* (TK001-t) cells and *trt1-myc pku70-d* (TK001-t7M) cells were cultured at 25 °C. PCRs were performed as in Fig. 4A.

Fig. 6. *dna2-C2* mutant is not sensitive to bleomycin or γ–rays at 25°C and 30°C. (**A**) The bleomycin sensitivities of wild-type cells (JY741), *rad50-d* (JY120), *dna2-C2* (HK10), and *rad50-d dna2-C2* (KT120n) cells were assayed by a spot test at 25°C and 30°C. (**B**) The sensitivities to γ–rays of wild-type cells (JY741), *rad50-d* (KT120), *dna2-C2* (HK10) at 25°C and at 30°C. The percent survival of the indicated strains was plotted versus the γ–ray dose. Standard deviations are shown by error bars.

Fig. 7. Model for the processing of telomere ends. (**A**) Comparison of models for the processing of Okazaki fragments and telomere ends. Dna2 can specifically cut the 5’ end during Okazaki fragment processing. Similarly, we assume that Dna2 specifically cuts C-rich

DNA after the telomere end is unwound by the Rad50 complex. Additional helicase activity may be required for unwinding of telomere ends. (**B**) Summary of the roles of Dna2, the Rad50 complex, and Ku heterodimer in telomere resectioning in *taz1-d* cells. In *taz1-d* cells, G-rich overhangs are significantly increased in a Rad50 complex-dependent manner, suggesting that Taz1 inhibits the Rad50 complex from performing the resection (59). The *taz1-d dna2-C2* double mutant has no overhang, suggesting that Dna2 is required for the resectioning. The *taz1-d rad50-d pku70-d* triple mutant has the overhang, but the *taz1-d dna2-C2 ku70-d* triple mutant does not have it, suggesting that Dna2 resects telomere ends without the assistance of the Rad50 complex in the absence of both Taz1 and Ku heterodimer. Our results suggest that Ku heterodimer inhibits Dna2 from performing the resectioning, but the Rad50 complex allows Dna2 to resect telomere ends in the presence of Ku heterodimer.

Table 1. Strains used in this study.

Strain	Genotype	source
JY741	*h⁻ leu1-32 ura4-D18 ade6-M216*	Lab stock
JY746	*h⁺ leu1-32 ura4-D18 ade6-M210*	Lab stock
KT001	*h⁻ leu1-32 ura4-D18 ade6-M216 taz1::ura4⁺*	Ref. 56
KT110	*h⁺ leu1-32 ura4-D18 ade6-M210 taz1::LEU2*	Ref. 56
KT021	*h⁻ leu1-32 ura4-D18 ade6-M216 rad50::LEU2 taz1::ura4⁺*	Ref. 56
KT00g	*h⁻ leu1-32 ura4-D18 ade6-M216 exo1::ura4⁺*	Ref. 56
KT01g	*h⁻ leu1-32 ura4-D18 ade6- taz1::LEU2 exo1::ura4⁺*	This work
YA132	*h⁻ leu1-32 ura4-D18 rad2::ura4⁺*	Iwasaki
KT11f	*h⁺ leu1-32 ura4-D18 ade6-M210 taz1::LEU2 rad2::ura4⁺*	This work
HK10	*h⁻ leu1-32 ura4-D18 dna2-C2*	Ref. 30
KT010n	*h⁻ leu1-32 ura4-D18 taz1::LEU2 dna2-C2*	This work
pku70A	*h⁺ leu1-32 ura4-D18 ade6-M210 pku70::LEU2::ade6*	Ref. 56
KT1105n	*h⁺ leu1-32 ura4-D18 ade6- dna2-C2 taz1:: LEU2 pku70::LEU2::ade6⁺*	This work
KT120	*h⁺ leu1-32 ura4-D18 ade6-M210 rad50::LEU2*	Ref. 56
KT120n	*h⁺ leu1-32 ura4-D18 rad50::LEU2 dna2-C2*	This work
Rad3D	*h⁻ leu1-32 ura4-D18 ade6-704 rad3::ura4⁺*	Ref. 58
KT104	*h⁺ leu1-32 ura4-D18 ade6-M210 rad3::ura4⁺*	This work
KT004n	*h⁻ leu1-32 ura4-D18 ade6-M210 dna2-C2 rad3::ura4⁺*	This work
709	*h⁺ leu1-32 ura4-D18 exo1::ura4⁺*	Ref. 56
KT10gn	*h⁺ leu1-32 ura4-D18 dna2-C2 exo1::ura4⁺*	This work
KTtnM	*h⁺ leu1-32 ura4-D18 ade6-M210 dna2-myc:kanMX*	This work
KTtnMM1	*h⁺ leu1-32 ura4-D18 dna2-C2-myc:kanMX*	This work
TKt7M	*h⁺ leu1-32 ura4-D18 ade6-M210 trt1-myc:kanMX*	This work
KT000n-t7M	*h⁻ leu1-32 ura4-D18 dna2-C2 trt1-myc:kanMX*	This work
LSP11	*h⁺ leu1-32 ura4-D18 cdc25-22*	Ref. 32
TK001-t	*h⁺ leu1-32 ura4-D18 cdc25-22 trt1-myc:kanMX*	This work
TK001-t7M	*h⁺ leu1-32 ura4-D18 pku70::LEU2 cdc25-22 trt1-myc:kanMX*	This work
KT146	*h⁻ leu1-32 ura4-D18 ade6-704 rad3::ura4⁺ rad32::ura4⁺*	This work

Fig1A

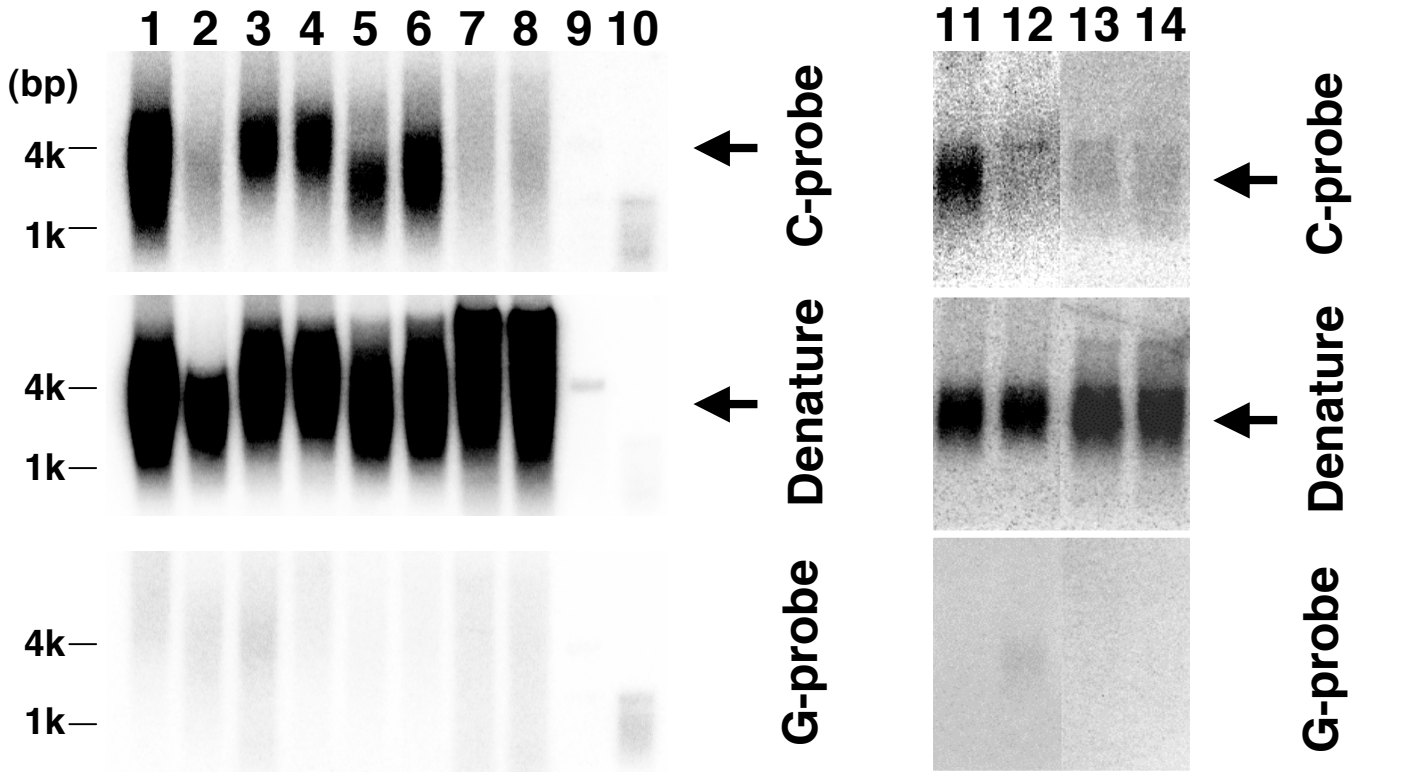
1 2 3 4 5 6 7 8 9 10
11 12 13 14
(bp)
4k
1k
C-probe
Denature
G-probe

B

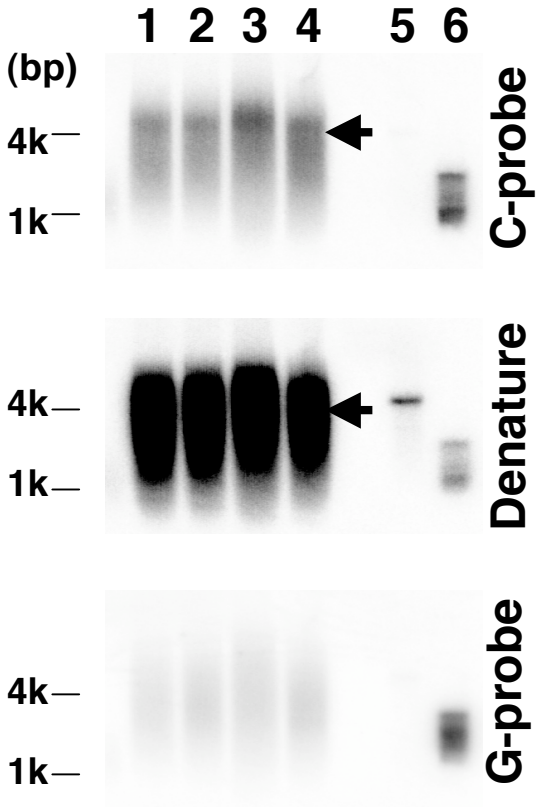
1 2 3 4 5 6
(bp)
4k
1k
C-probe
Denature
G-probe

C

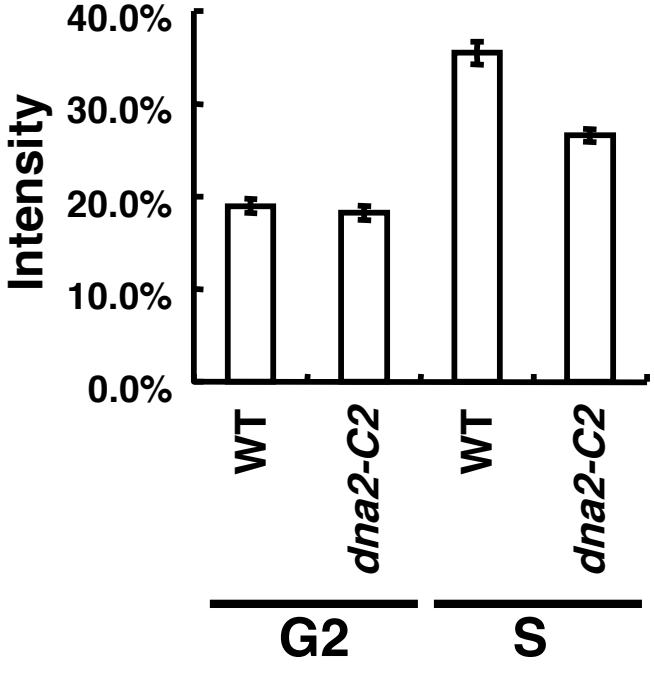
Intensity
40.0%
30.0%
20.0%
10.0%
0.0%
WT
dna2-C2
WT
dna2-C2
G2
S

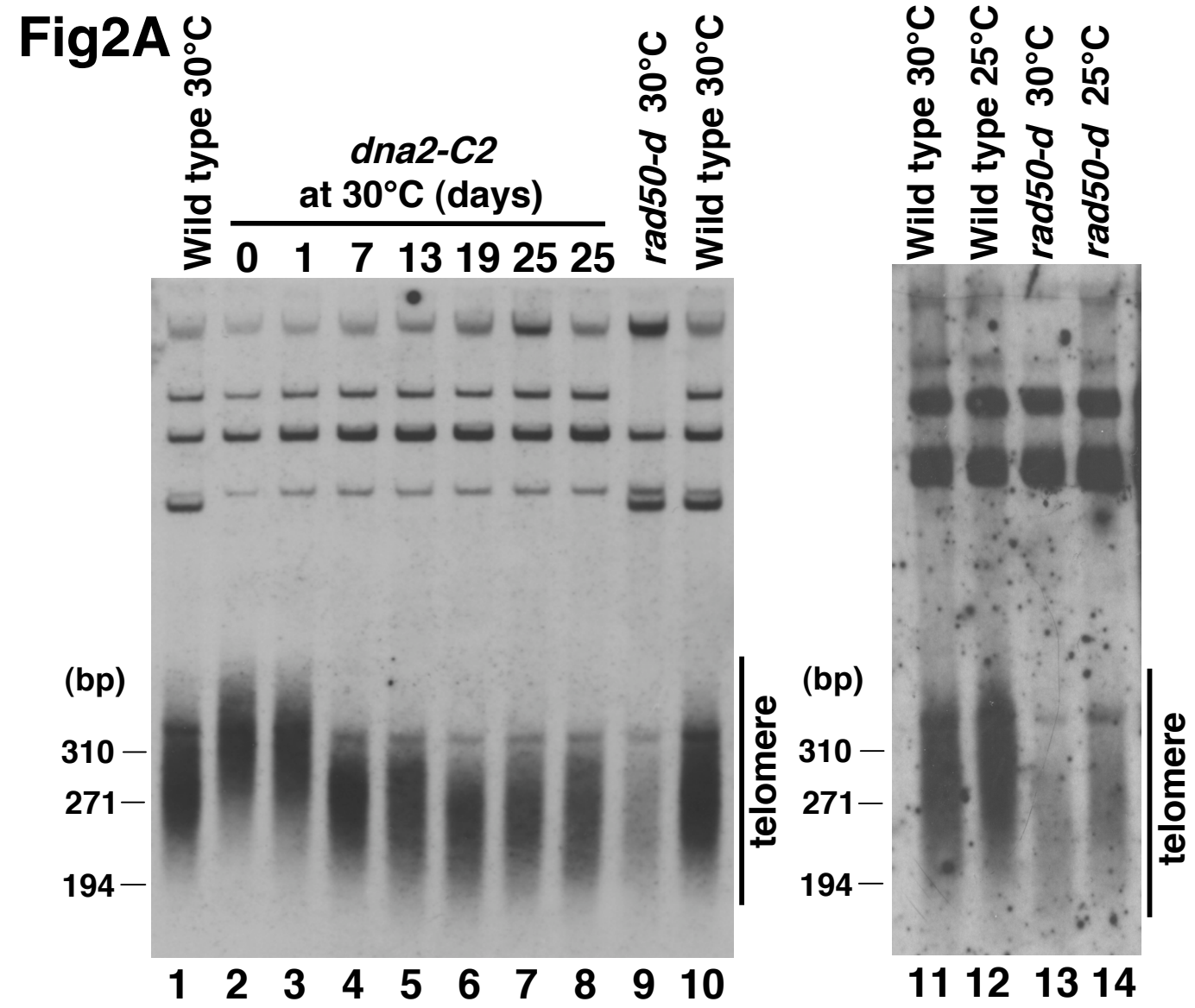
Fig2A
Wild type 30°C
dna2-C2
at 30°C (days)
0 1 7 13 19 25 25
rad50-d 30°C
Wild type 30°C
Wild type 30°C
Wild type 25°C
rad50-d 30°C
rad50-d 25°C
(bp)
310
271
194
telomere
(bp)
310
271
194
telomere
1 2 3 4 5 6 7 8 9 10
11 12 13 14

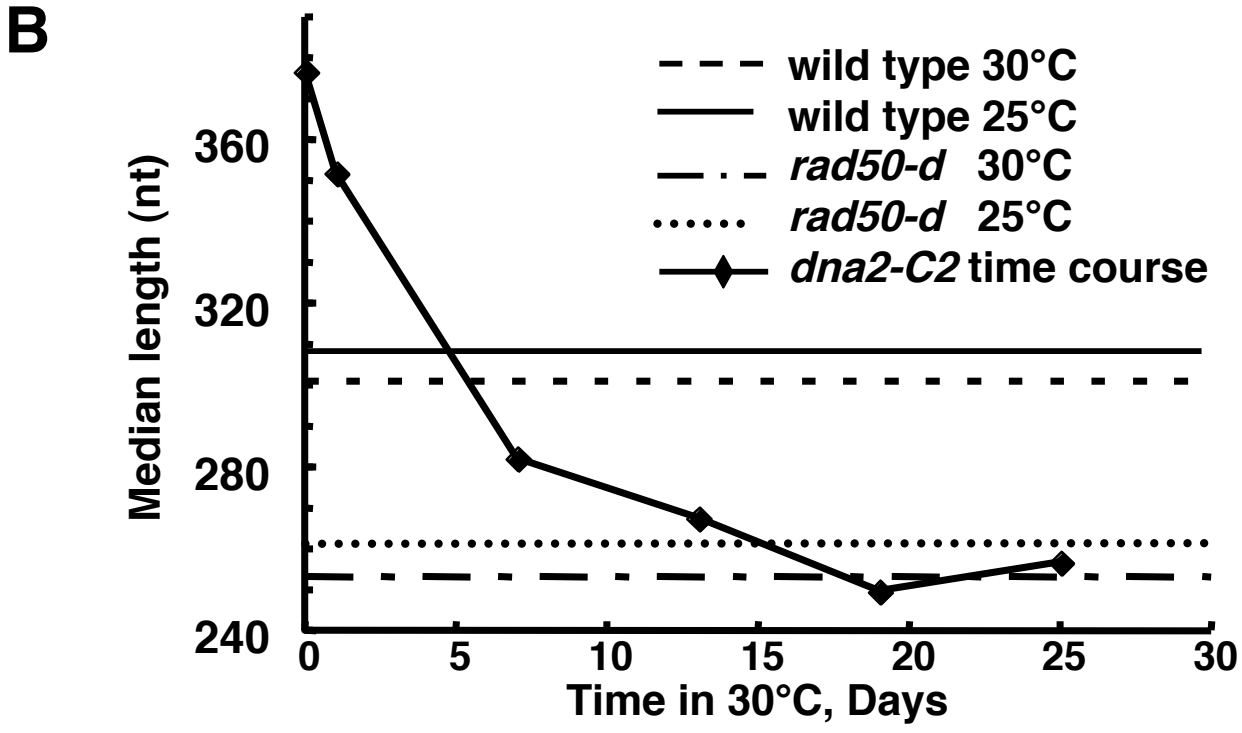
B
wild type 30°C
wild type 25°C
rad50-d 30°C
rad50-d 25°C
dna2-C2 time course
Median length (nt)
360
320
280
240
0
5
10
15
20
25
30
Time in 30°C, Days

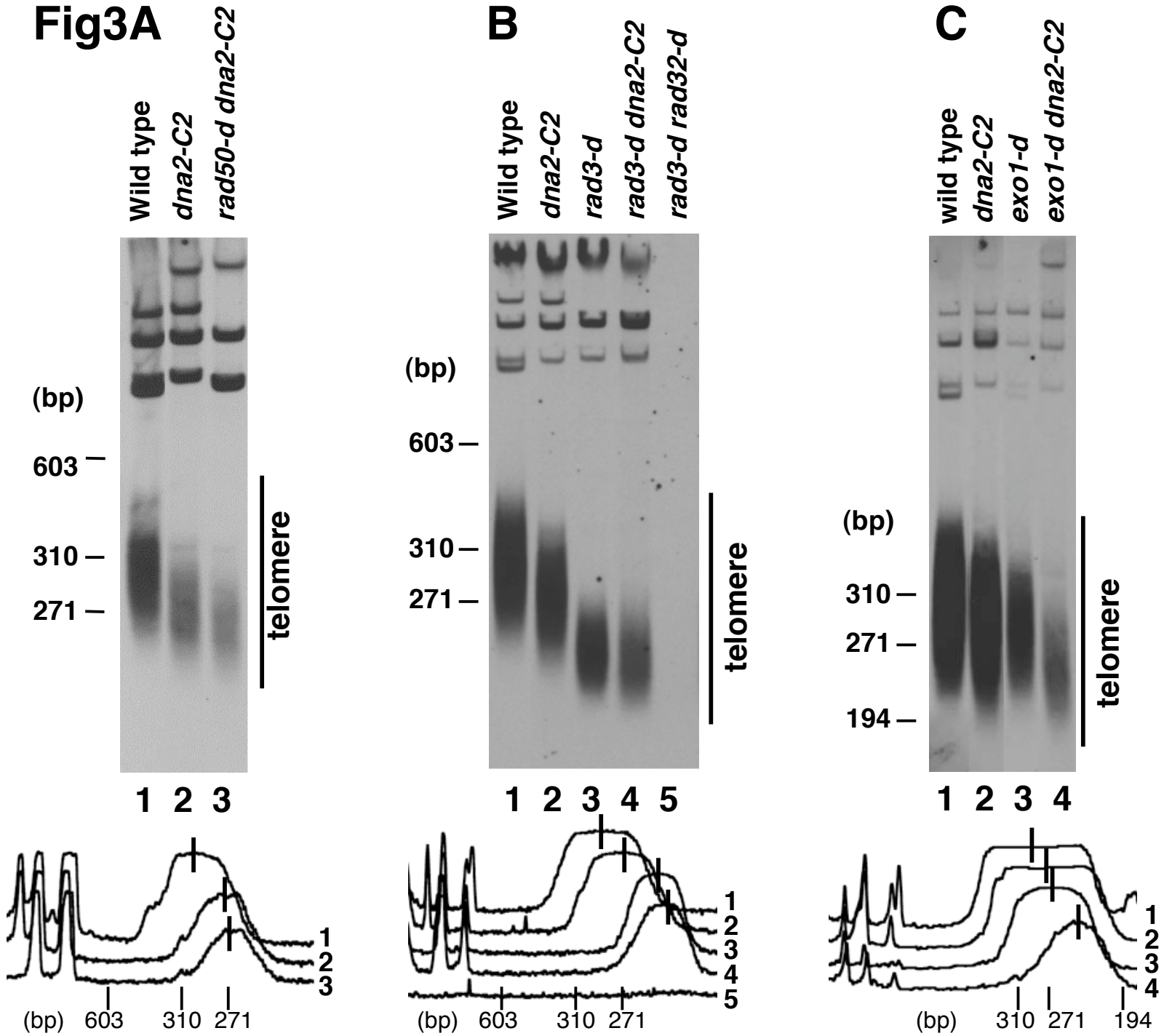
Fig3A
Wild type
dna2-C2
rad50-d dna2-C2
(bp)
603
310
271
telomere
1 2 3
(bp) 603 310 271
1
2
3
B
Wild type
dna2-C2
rad3-d
rad3-d dna2-C2
rad3-d rad32-d
(bp)
603
310
271
telomere
1 2 3 4 5
(bp) 603 310 271
1
2
3
4
5
C
wild type
dna2-C2
exo1-d
exo1-d dna2-C2
(bp)
310
271
194
telomere
1 2 3 4
(bp) 310 271 194
1
2
3
4

Fig4A

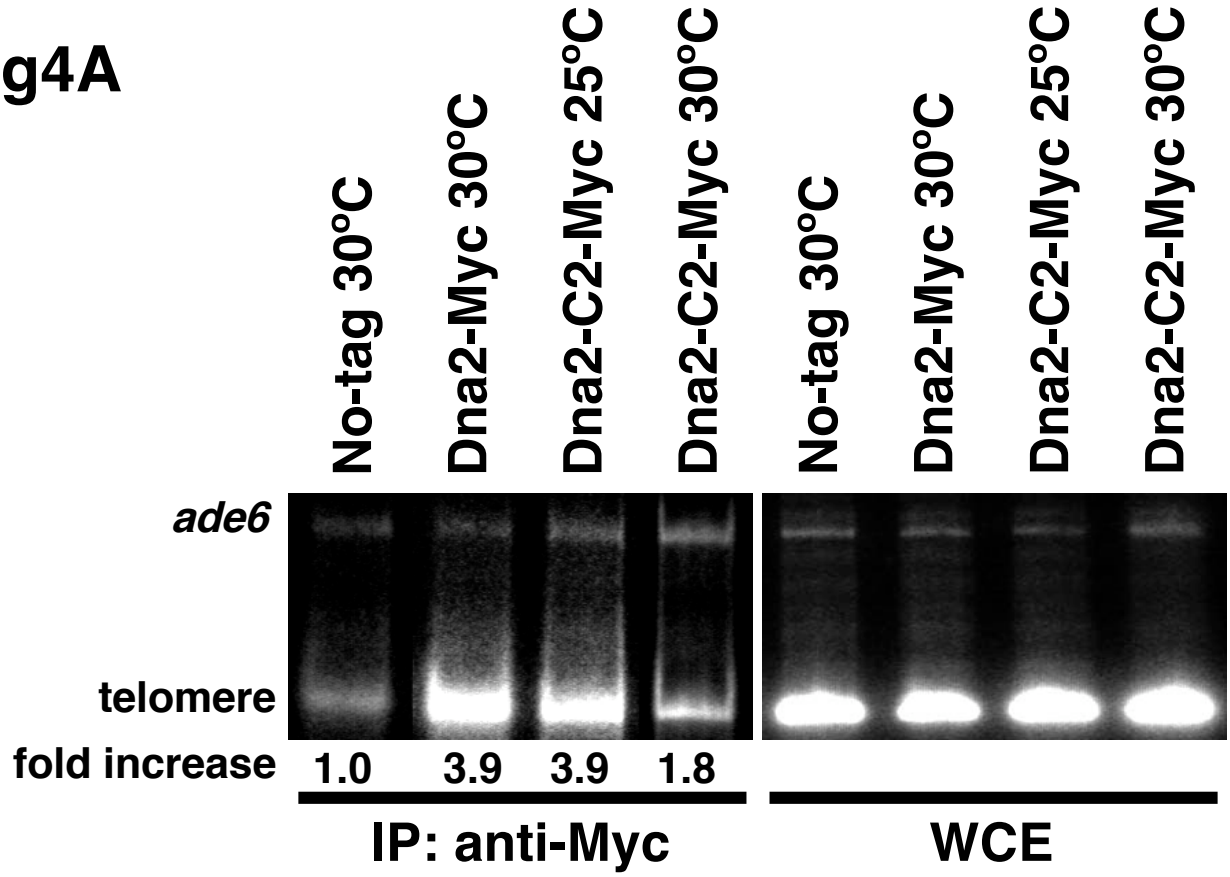
No-tag 30°C
Dna2-Myc 30°C
Dna2-C2-Myc 25°C
Dna2-C2-Myc 30°C
No-tag 30°C
Dna2-Myc 30°C
Dna2-C2-Myc 25°C
Dna2-C2-Myc 30°C
ade6
telomere
fold increase
1.0
3.9
3.9
1.8
IP: anti-Myc
WCE

B

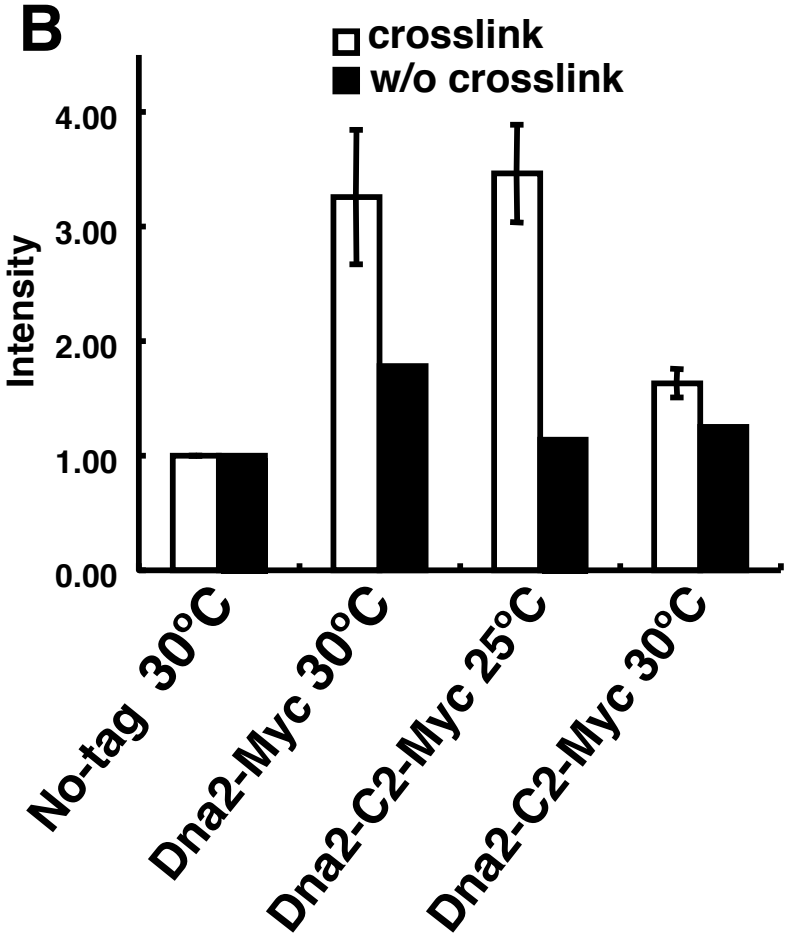
crosslink
w/o crosslink
Intensity
4.00
3.00
2.00
1.00
0.00
No-tag 30°C
Dna2-Myc 30°C
Dna2-C2-Myc 25°C
Dna2-C2-Myc 30°C

C

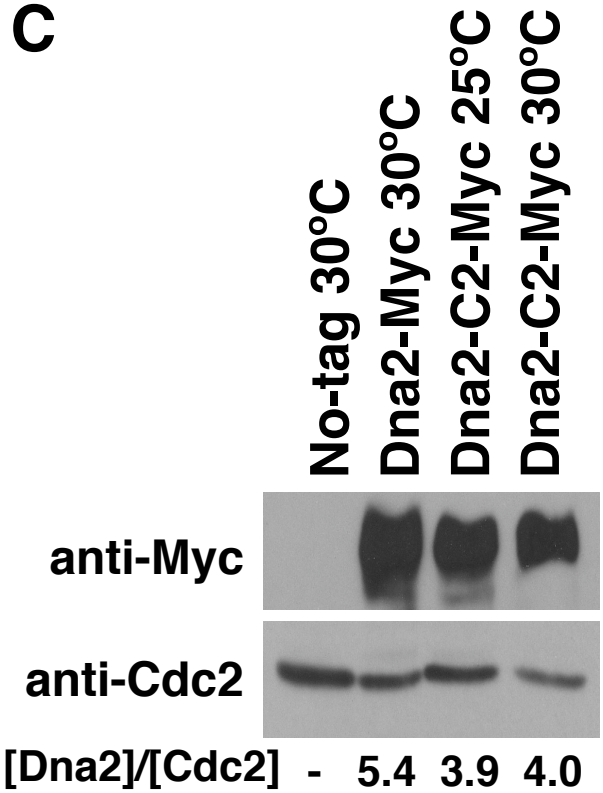
No-tag 30°C
Dna2-Myc 30°C
Dna2-C2-Myc 25°C
Dna2-C2-Myc 30°C
anti-Myc
anti-Cdc2
[Dna2]/[Cdc2]
-
5.4
3.9
4.0

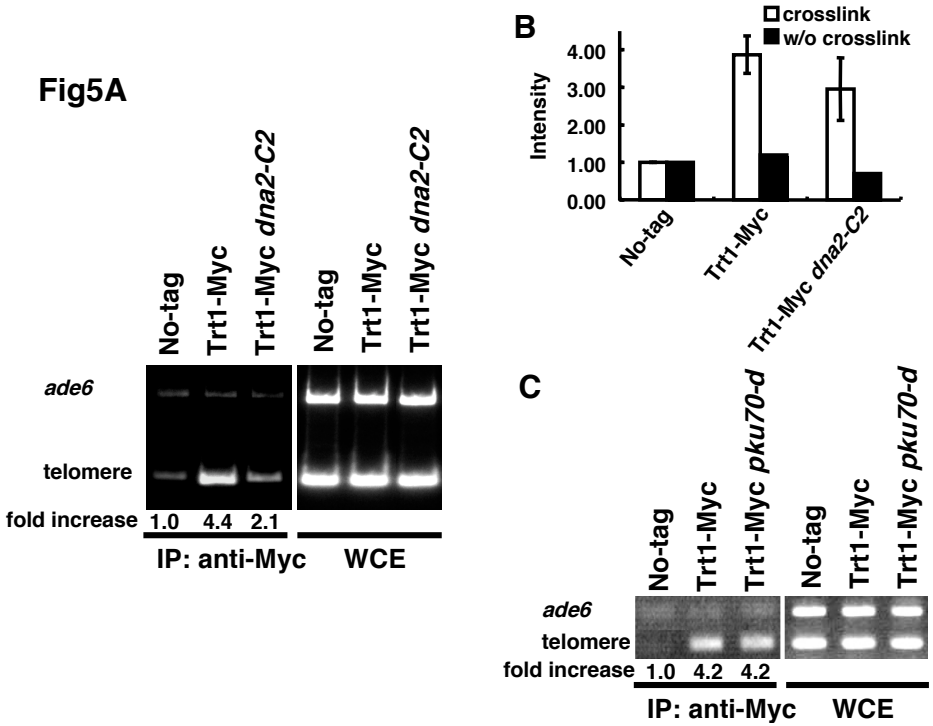
Fig5A
No-tag
Trt1-Myc
Trt1-Myc dna2-C2
No-tag
Trt1-Myc
Trt1-Myc dna2-C2
ade6
telomere
fold increase
1.0
4.4
2.1
IP: anti-Myc
WCE
B
crosslink
w/o crosslink
Intensity
4.00
3.00
2.00
1.00
0.00
No-tag
Trt1-Myc
Trt1-Myc dna2-C2
C
No-tag
Trt1-Myc
Trt1-Myc pku70-d
No-tag
Trt1-Myc
Trt1-Myc pku70-d
ade6
telomere
fold increase
1.0
4.2
4.2
IP: anti-Myc
WCE

Fig6A

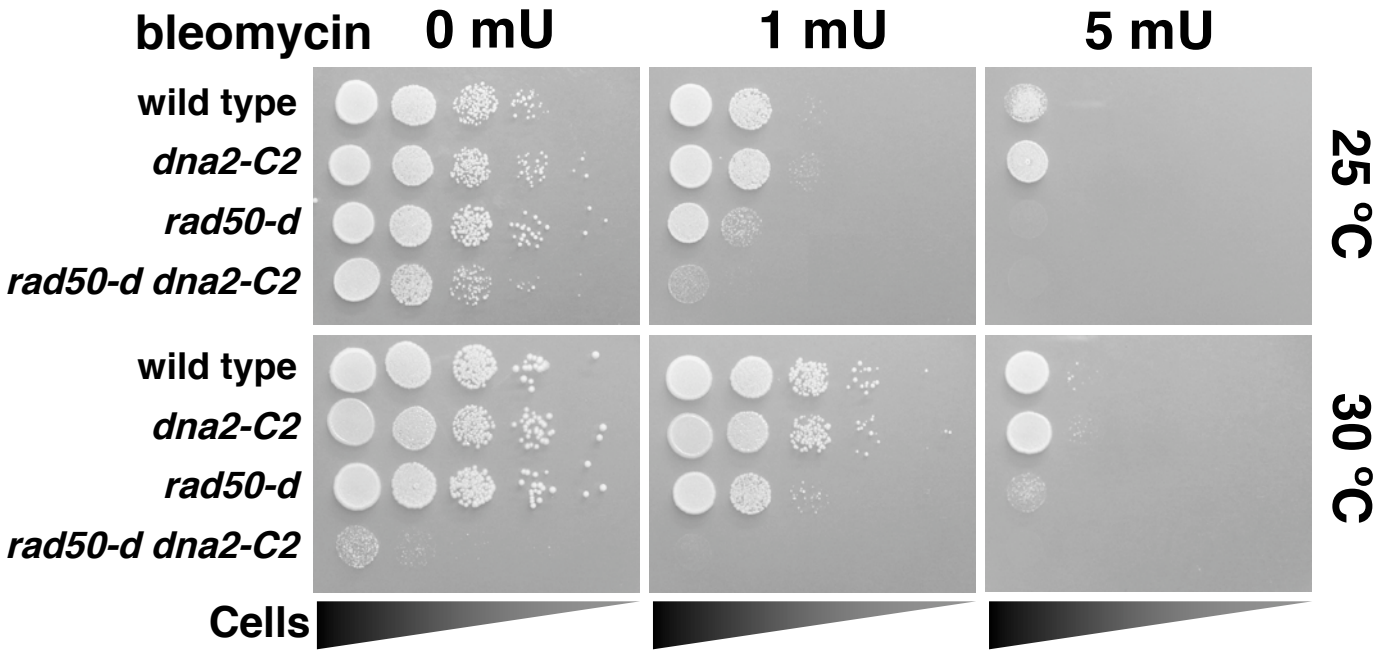
bleomycin
0 mU
1 mU
5 mU
wild type
dna2-C2
rad50-d
rad50-d dna2-C2
25 °C
wild type
dna2-C2
rad50-d
rad50-d dna2-C2
30 °C
Cells

B

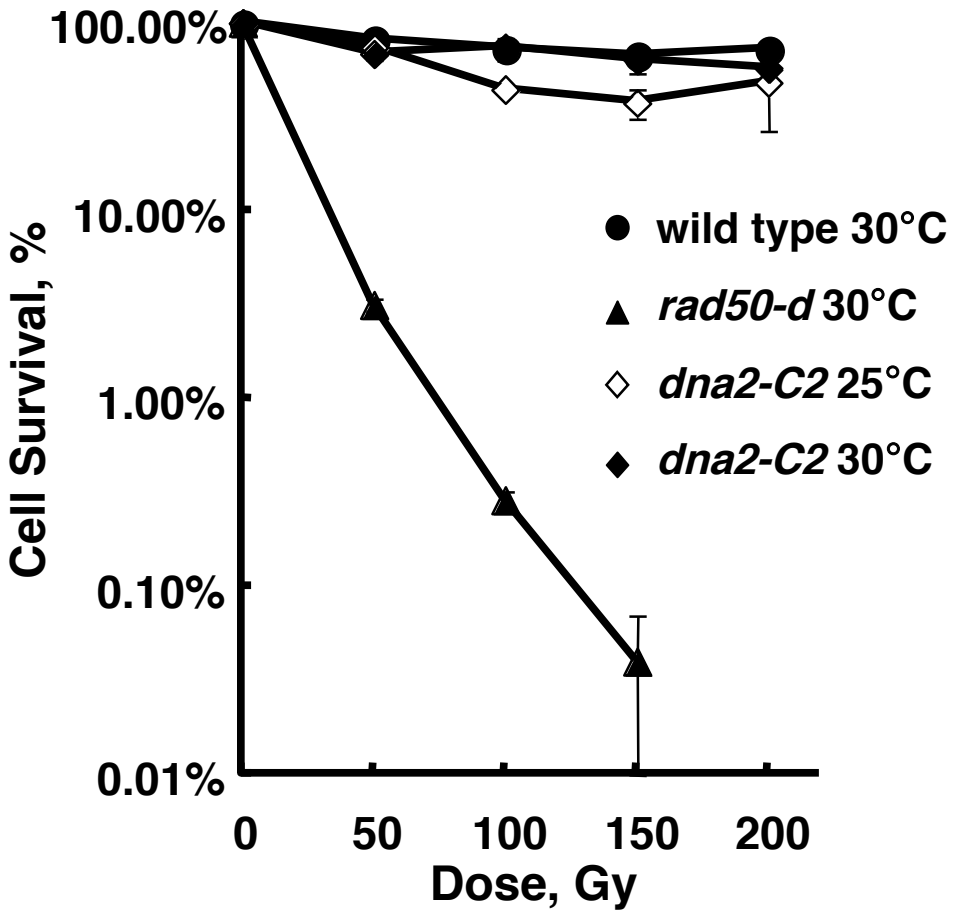
100.00%
10.00%
1.00%
0.10%
0.01%
Cell Survival, %
0
50
100
150
200
Dose, Gy
wild type 30°C
rad50-d 30°C
dna2-C2 25°C
dna2-C2 30°C

Fig7

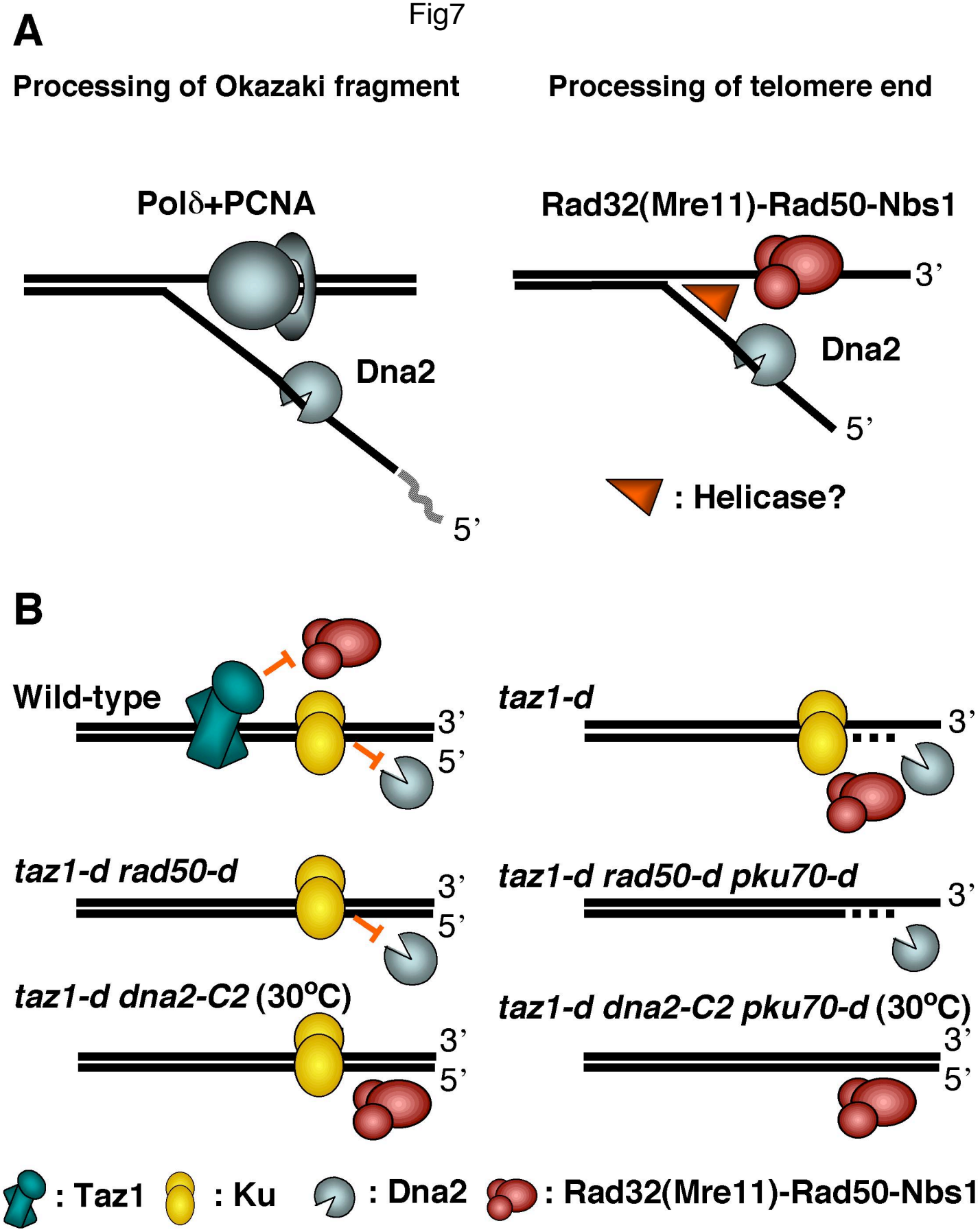
A
Processing of Okazaki fragment
Processing of telomere end
Polδ+PCNA
Dna2
5'
Rad32(Mre11)-Rad50-Nbs1
3'
Dna2
5'
: Helicase?
B
Wild-type
3'
5'
taz1-d
3'
taz1-d rad50-d
3'
5'
taz1-d rad50-d pku70-d
3'
taz1-d dna2-C2 (30°C)
3'
5'
taz1-d dna2-C2 pku70-d (30°C)
3'
5'
: Taz1
: Ku
: Dna2
: Rad32(Mre11)-Rad50-Nbs1